EFSUMB Course Book, 2nd Edition

Editor: Christoph F. Dietrich

Ultrasound of the salivary glands and soft tissue lesions of the neck

Norbert Gritzmann[1], Susanne A. Quis[1], Rhodri M. Evans[2]

[1]SONOSEMINARE, Austria.

[2]Swansea University Medical School, Abertawe Bro Morgannwg University LHB, Wales.

Corresponding author[1]:

Univ. Prof. Dr. Norbert Gritzmann

SONOSEMINARE

1190 Vienna, Strehlg.13 B 8

Austria

Tel: (+) 43 676 84 04 64

Fax: (+) 43 676 84 04 64

Email: norbert.gritzmann@gmail.com

Topography and sonographic anatomy of the salivary glands

The three pairs of salivary glands can be easily identified within the neck using ultrasound. The parotid gland is located in the retromandibular fossa as a triangular, echogenic structure. The submandibular gland is situated under the body of the mandible, abutting the posterior free edge of the mylohyoid muscle. The sublingual glands lie deep to the mylohyoid muscle, they are identified in the sublingual space lying lateral to the genioglossus muscle.

Sonographic anatomy

Parotid gland

Sonographically, the parotid gland is a triangular, uniformly hyperechoic structure in the retromandibular fossa [Figure 1].

Figure 1 Transverse section of the normal left parotid gland.

The majority of the parotid gland can be easily assessed by ultrasound; however, the deep portion of the gland may be difficult to visualise and the portion of the parotid gland which lies medial to the mandible cannot be identified consistently. The masseter muscle is located deep to the anterior part of the superficial parotid, lateral to the ramus of the mandible. The inferior portion of the parotid gland may be referred to as the cervical lobe. Within the

parenchyma, the retromandibular vein is often identified lying lateral to the external carotid artery. The plane of the retromandibular vein through the parotid can be used to differentiate between the superficial and deep part of the parotid gland [(1)]. Small, bean-shaped or oval, hypoechoic structures within the gland are commonly identified, they represent reactive, hyperplastic lymph nodes.

Normal minor, peripheral, nondilated intraglandular ducts are not visualised by ultrasound. The main duct (Stensen's duct) is sonographically identifiable as either a tubular structure using high resolution transducers (>10 MHz) or is identified as a single echogenic line. The facial nerve is not visualised sonographically [(2)].

Submandibular gland

The submandibular gland is triangular shaped with a homogeneous echogenic structure, identified at the posterior border of the mylohyoid muscle. The facial artery and vein are located posterior to or within the gland, the facial artery passing superiorly behind the submandibular gland, over the inferior body of the mandible. Nondilated intraglandular ducts are usually not identified, but may be seen as faintly visible narrow, confluent tubules. Wharton's duct (main duct) is identified between the mylohyoid and hyoglossus muscles, colour flow imaging may help in differentiating it from the adjacent lingual vessels.

Sublingual gland

Sonographically the sublingual gland is distinguished from the genioglossus muscles as an echogenic mass lying lateral to the genioglossus, deep to the mylohyoid. There may be a direct communication with the submandibular gland situated dorsally. The ducts lead to the sublingual caruncle in the anterior part of the floor of the mouth which cannot be identified with ultrasound.

Colour Duplex Doppler

Salivary glands are well perfused. Their arterial supply and associated veins can be displayed by colour Doppler sonography. The retromandibular vein can be used to differentiate superficial and deep lesions of the parotid gland (venous plane). Colour Doppler sonography is used to assess the vascularisation of salivary gland diseases [(3)]. It is not possible to use

colour flow patterns or specific Doppler characteristics to diagnose specific pathological entities within the salivary glands. However, the peak systolic velocity of the intraparenchymal arteries increases after stimulation (vitamin C or lemon stick). The lack of a detectable increase in peak systolic velocity after stimulation can be used in the assessment of Sjögren's syndrome.

Pathological changes in the salivary glands

Acute inflammation of the salivary glands

Acute bacterial sialadenitis usually arises as a consequence of a bacterial, ductogenic, ascending infection and often affects older patients [Figure 2].

Figure 2 Enlarged submandibular gland. Hypervascularisation is visualised on power Doppler. Typical inflammation of the submandibular gland is visualised.

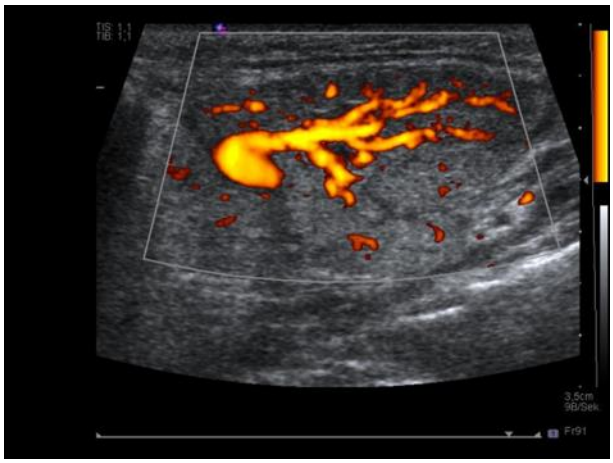

The main indication for ultrasound is to assess whether an obstructive sialadenitis with ductal dilatation is present or whether there is a cystic mass, i.e. abscess formation. Enlarged, intraglandular, hypoechoic lymph nodes should not be confused with small abscesses. The oval shape of the lymph nodes and their eccentric echogenic hilum with its associated hilar blood flow pattern helps with identification. Purulent abscess formation can

present as a heterogeneous mass or is sometimes identified as a frankly cystic collection. Pus within an abscess can be relatively echogenic.

Colour Doppler sonography demonstrates a reactive hypervascularity in the surrounding parenchyma. Using palpation under sonographic control (sonopalpation), motion of the pus/debris within the abscess can occasionally be visualised. Ultrasound contrast media can be used to delineate the liquefaction of an abscess. Ultrasound guided aspiration can prove or exclude the diagnosis of an abscess. The ability to obtain accurate microbiology can aid management. Viral infections, such as mumps, usually show bilateral hypoechoic enlargement of the parotid glands. Typically hypervascularity is found on colour Doppler sonography. CEUS can help in the early diagnosis of non-vascularised abscesses.

Chronic inflammation of the salivary glands

Chronic (recurrent) sialadenitis

Chronic sialadenitis typically presents unilaterally, underlying causes include recurrent bacterial infection. Strictures or stenoses of the ducts may be precipitating factors. The gland is less swollen than in acute sialadenitis and is heterogeneous in appearance. Duct dilatation may be detected. Salivary duct strictures are more accurately visualised by sialography than by ultrasound. Ultrasound is used primarily to exclude a causal sialolithiasis [Figure 3].

Intra- or periglandular, moderately enlarged lymph nodes with hyperechoic hila can be detected in chronic sialadenitis. In children, chronic cystic parotitis can be diagnosed sonographically with small hypoechoic lesions visualised within the echogenic parenchyma. Usually this condition is self-limiting.

Küttner’s tumour is a chronic sclerosing sialadenitis of the submandibular gland. Typical appearances are those of an ill-defined, heterogeneous submandibular gland. Special care should be taken to recognise the intraglandular ducts and vessels in order not to confuse the abnormal submandibular gland with a tumour. Sclerosing sialadenitis may affect the submandibular gland partially. Hypoechogenic areas are visualised within the submandibular gland.

Figure 3 Left parotid gland in a child. Multiple cystic lesions are detected in a gland with a background of normal echogenic parenchyma. Chronic cystic parotitis was diagnosed.

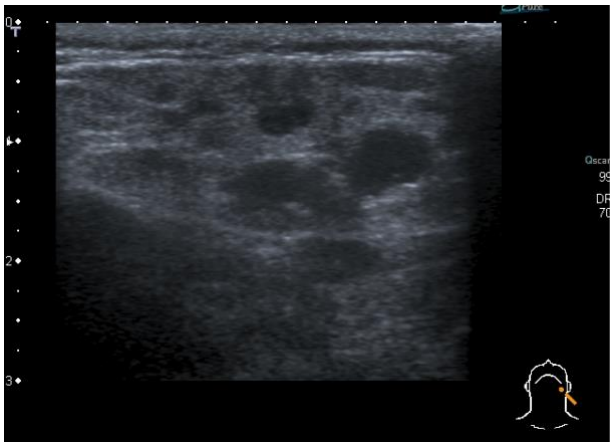

Sjögren's syndrome

Sjögren's syndrome is an autoimmune disease. The clinically significant xerostomia is caused by a myoepithelial sialadenitis with fibrosis. The changes are seen in the parotid and submandibular glands. Chronic sialadenitis and Sjögren's syndrome demonstrate a similar appearance sonographically, however chronic sialadenitis is usually unilateral whereas Sjögren's affects the salivary glands symmetrically. The glands are enlarged, heterogeneous in echotexture, with multiple small hypoechoic areas within. The appearances are sometimes likened to a ‘currant cake’ or ‘leopard skin’ appearance [Figure 4] [(4)].

Enlarged intra- or extraglandular lymph nodes are a frequent finding in Sjögren's syndrome. If an enlarged lymph node mass is identified then biopsy should be considered because there is an increased risk of non-Hodgkin lymphoma in Sjögren's syndrome. It is recommended that when a hypoechogenic mass of more than 1 cm is identified within a salivary gland that displays signs of Sjögren's syndrome, a histological evaluation should be performed.

Figure 4 Transverse section of the right parotid gland in a patient with Sjögren's syndrome. The gland is markedly hypoechogenic with multiple hypoechoic areas, moderate hypervascularisation is present.

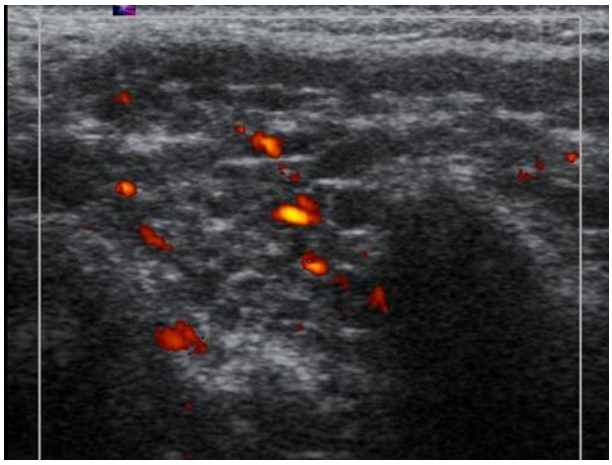

Colour Doppler shows increased blood flow during the acute stages of inflammation. However, during the fibrous stages of the disease, the blood flow measured by peak systolic velocities in pulsed Doppler sonography does not increase after stimulation with a lemon stick or Vitamin C.

Epithelioid sialadenitis

Epithelioid cell (granulomatous) inflammation of salivary glands with intra- and periglandular lymph nodes is an extrapulmonary manifestation of sarcoidosis. In sarcoid infiltration, symmetrical, enlarged parotid glands can be found. Typically, the enlarged salivary glands are painless and contain multiple small nodules within. A facial palsy or fever may be present. Hypoechoic lymph nodes or intraglandular hypoechoic conglomerates may be identified. The appearances can mimic chronic infection or lymphoma.

Tuberculosis of the salivary glands

Tuberculosis of the salivary glands often exhibits a pseudotumourous appearance in sonography. Parotid tuberculosis may be confused with a malignant, ill-defined hypoechogenic tumour. Therefore, histological evaluation is usually recommended. The

diagnosis can be made with the detection of acid-fast bacilli in the parotid biopsy sample [(5)].

Post-radiotherapy sialadenitis

Following irradiation of head and neck cancers, there is often an associated sialadenitis. Sonographically in the acute stage, the glands are diffusely hypoechoic and are often moderately enlarged. In the chronic form the gland is small and frequently ill-defined, i.e. poorly demarcated from the surrounding soft tissues. Ultrasound can be very useful in providing diagnostic information in submandibular masses post-radiotherapy in patients who have been treated for head and neck cancer. It can differentiate between lymph node recurrence and post-radiotherapy sialadenitis.

Sialolithiasis

Salivary gland calculi are distributed primarily within the submandibular gland and its associated Wharton's duct (more than 80% of patients). In approximately 10% of patients, the stones are found in the parotid gland or in the associated Stensen's duct. Salivary calculi of the sublingual gland are rare. Symptomatic salivary stones occur when there is an obstruction of the ductal system. The key feature to elicit is whether there are stones within the main duct of the salivary glands, within the small intraglandular ducts or within the salivary gland parenchyma. Common sites are the genu of the main submandibular gland (the bend that occurs as the duct passes around the posterior border of the mylohyoid) or within the intraglandular ducts of the submandibular gland [(2)].

Calculi of the parotid gland usually arise in the periphery of the duct system or within the glandular parenchyma. Salivary stones are typically echogenic structures with posterior acoustic shadowing [Figures 5 and 6]. In cases of very small stones (<2-3 mm) the posterior shadowing may be absent or may be weak. In symptomatic sialolithiasis there is usually an accompanying ductal dilatation and sonographically evident inflammatory change within the salivary gland.

Figure 5 Longitudinal section of the submandibular duct, a stone is visualised.

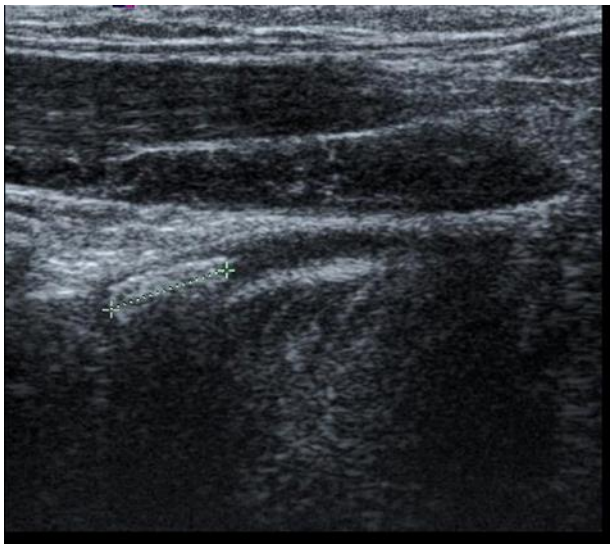

Figure 6 Longitudinal section of a moderately dilated submandibular duct (Wharton's duct). A stone is located in the anterior portion of the duct.

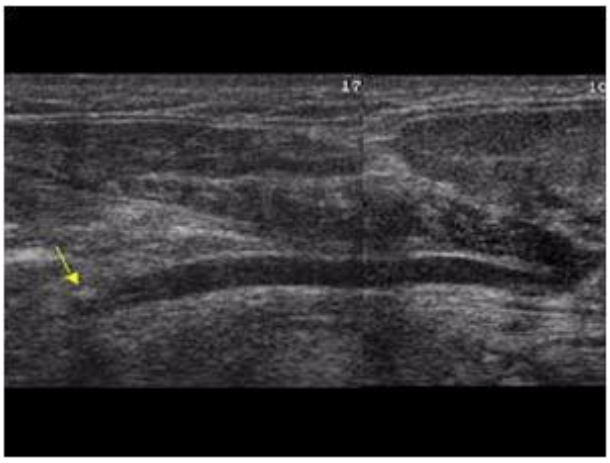

Figure 7 Oral ultrasound with a small footprint transducer shows a dilated echogenic duct with an obstructing stone.

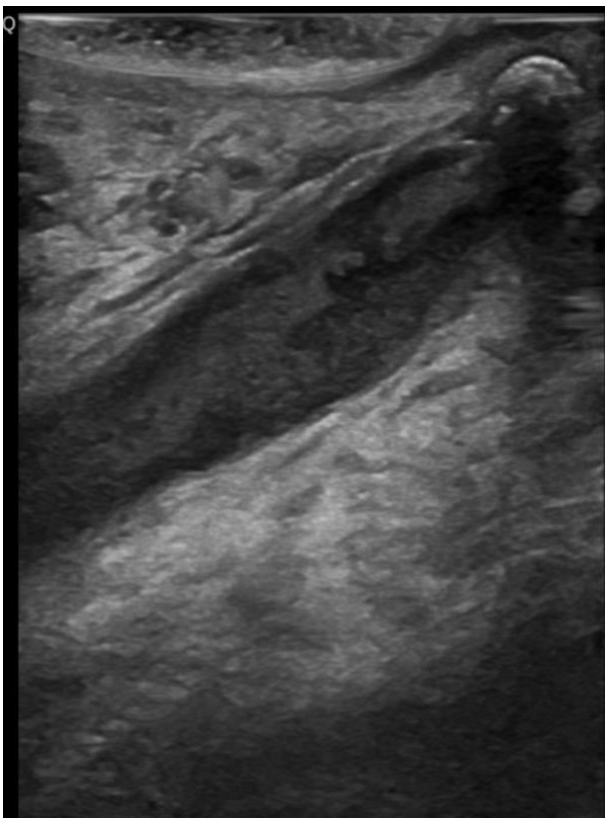

Ductal dilatation is visualised as a tubular, hypoechoic branching of the intraglandular ducts [Figure 7]. Associated inflammatory changes result in hypoechoic swelling of the gland. Ultrasound is a sensitive imaging modality in the detection of salivary stones with quoted accuracies of 90%. About 20% of salivary stones are radiolucent on radiography, with ultrasound it is possible to identify these stones and to identify their precise location. In experienced hands, ultrasound is now the primary imaging method for sialolithiasis.

Tumours of the salivary glands

About 95% of salivary gland tumours are primarily epithelial in origin. Salivary tumours are predominantly benign (80%). About 70% of the tumours are located in the parotid gland, 10% in the submandibular gland and the remainder in the sublingual and minor salivary glands. The size of the salivary gland is inversely related to the likelihood of any tumour detected being malignant, i.e. if a tumour is detected in a sublingual gland there is a higher

probability that this tumour is malignant compared to a tumour detected in the larger parotid gland [(2)].

Pleomorphic adenoma

Pleomorphic adenomas are the most common salivary tumour, they are also known as mixed cell tumours. The parotid gland is the most common location of the mixed cell tumour and about 60% of all parotid gland tumours are mixed cell tumours. They are benign and often slow growing tumours. Frequently patients present with findings of a firm mass in the parotid gland which has been present for many years. Women are affected slightly more often than men. Clinically, the findings are of a firm, nodular, painless mass. Most tumours are superficial to the facial nerve, which is not infiltrated. So-called 'Iceberg tumours', which are tumours which arise within the deep portion of the parotid gland and extend into the parapharyngeal space, may cause swallowing problems. Sonographically, mixed tumours are homogeneous and relatively hypoechoic. They have a so-called 'pseudocystic' appearance with enhanced sound wave transmission and identifiable posterior acoustic shadowing. They are sharply bordered with an often lobulated contour, this is regarded as a typical finding [Figure 8]. Rarely, cystic change and areas of calcification can be identified. In long standing cases, malignant transformation is possible.

Figure 8 Longitudinal scan of the parotid gland. A sharply bordered hypoechoic lesion is visualised in the superficial portion of the parotid gland. A pleomorphic adenoma was diagnosed (note the pseudocystic appearance with acoustic enhancement identified deep to the tumour).

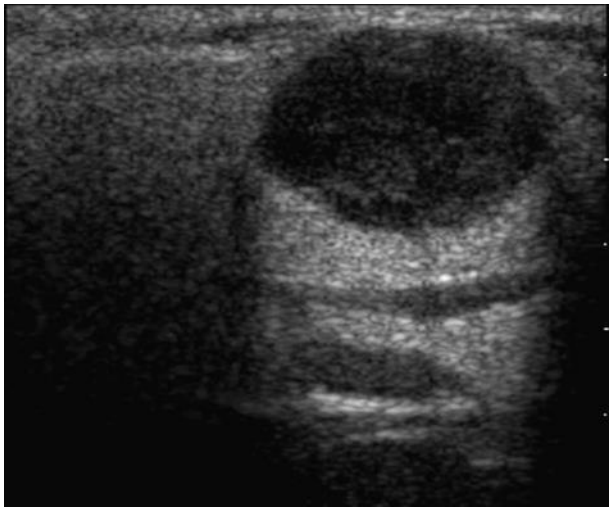

Adenolymphoma (Wharthin's tumour)

Adenolymphoma (also known as cystadenolymphoma) is the second most common, benign salivary gland tumour. In 90% of cases they are located in the superficial parotid gland, often in the caudal portion or tail of the gland. The tumours predominantly affect males, typically presenting in older men. Adenolymphoma is usually a softer, partially cystic, ovoid mass compared to pleomorphic adenoma. Histologically, the tumour is composed of epithelial glandular tissue with prominent associated lymphoreticular tissue. In up to 30%, a multilocular tumour may be present. In approximately 10 to 15% of cases the tumour may be bilateral. Sonographically, the tumours are sharply bordered, i.e. well-defined, hypoechoic and frequently contain a cystic component [Figure 9]. They are usually ovoid in shape and may contain areas of calcification.

Figure 9 Transverse section of the caudal part of the parotid gland. A sharply bordered hypoechogenic lesion with cystic parts is visualised. An adenolymphoma was diagnosed on histology.

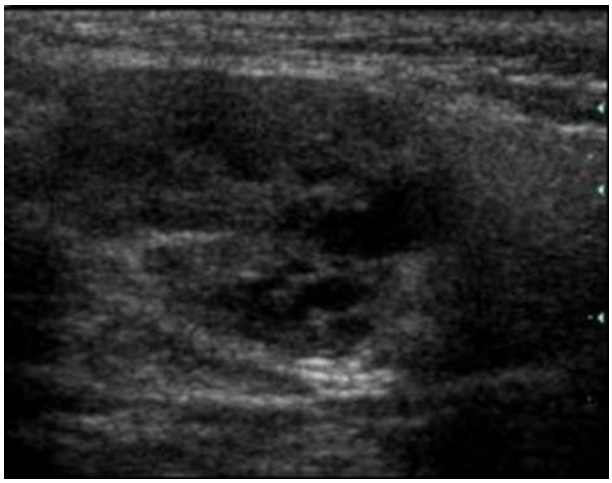

Non-epithelial tumours of the salivary glands

Within this relatively rare group of tumours (5% of salivary tumours), lymphangiomas and haemangiomas make up just over 50%. Haemangiomas are also classified as venous vascular malformations. On ultrasound, haemangiomas are typically well defined, hypoechoic lesions that may be compressible. The echostructure of haemangiomas depends on the size of the lacunar spaces which may vary considerably. The majority of haemangiomas are hypoechoic compared to the surrounding soft tissues.

Arteriovenous malformations display colour flow and arterial Doppler signal and they may be highly vascular lesions, especially when arteriovenous shunts are present. In thrombosed vascular malformations and in low flow lesions no colour flow may be identified.

The cystoid lymphangiomas demonstrate no vascularisation.

A lipoma is typically ovoid in shape, usually moderately compressible and has the classical feathered echostructure of adipose tissue. Fine echogenic striae are identified within the mass and are typically orientated parallel to the transducer [Figure 10] [(6)].

Figure 10 Transverse section of the parotid gland. A hypoechoic lesion with echogenic striae within is visualised in the parotid gland. Parotid lipoma was diagnosed on CT. A lesion with feathered structure is seen: Typical lipoma of the parotid gland.

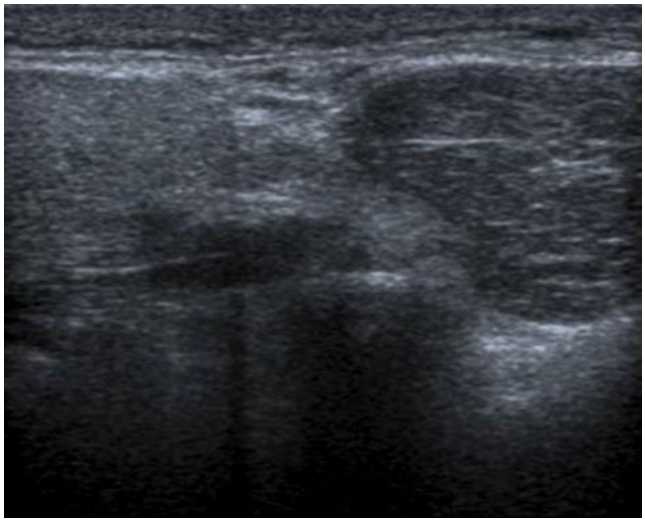

Lipomas are commonly located in the parotid area. The higher the fibrous content of the lipoma, the greater the echogenicity detected on ultrasound. Pure lipomas are relatively hypoechoic. The remaining non-epithelial salivary tumours are schwannomas and neurofibromas (about 7% of non-epithelial salivary gland tumours are sarcomas).

Epithelial, malignant tumours of the salivary glands

Carcinoma represents approximately 86% of malignant salivary tumours. Adenoid cystic carcinoma (formerly called cylindroma) is the most common carcinoma of the salivary glands (35%). Adenoid cystic carcinoma occurs relatively frequently in the minor salivary glands of the palate and pharynx. Sonographically, the tumour is usually a well-defined, round, hypoechoic mass [Figure 11].

Figure 11 Longitudinal section of the floor of the mouth. A slightly ill-defined lesion is seen in the region of the sublingual gland. Adenoid cystic carcinoma was diagnosed histologically.

In about 20% of the tumours, the margin is ill-defined and irregular. Histology often demonstrates perineural infiltration which cannot be shown by sonography. If a malignant salivary gland tumour is suspected either on ultrasound criteria or on cytology following an ultrasound guided biopsy, other imaging modalities such as CT or MRI may be indicated. In particular, if ultrasound is unable to define the extent of the mass, particularly if it is extending into the deep part of the parotid, further imaging e.g. MRI is indicated to define any extension into the parapharyngeal space. This cannot be detected with ultrasound.

Acinus cell carcinoma (3% of parotid gland tumours) is typically round in outline and possesses a pseudocapsule which manifests itself on ultrasound as a well-defined margin, i.e. it may have the same ultrasound appearances as a pleomorphic adenoma. A low grade, malignant, mucoepidermoid carcinoma, preferentially located in the parotid gland, may also exhibit the same appearances.

Mucoepidermoid carcinoma accounts for approximately 30% of all malignant salivary gland tumours. High grade mucoepidermoid carcinomas are usually ill defined lesions whereas low grade tumours may present as a sharply bordered benign looking tumour on imaging.

Intraglandular metastases

Tumours of the skin in the facial region and scalp e.g. squamous cell carcinoma, may metastasise to lymph nodes within the parotid gland. In malignant melanoma of the scalp, metastases to the lymph nodes of the parotid gland are frequently found. Squamous cell carcinoma metastases may exhibit necrosis within the intraparotid lymph nodes. Melanoma metastases typically present as rounded, hypoechoic lymph nodes within the parotid gland. Systemic diseases such as lymphoma will also manifest themselves as intraparotid lymphadenopathy. Typically, multiple conglomerates of hypoechoic masses are found in the parotid gland. If a central hilum is present, this may help to identify these as intraparotid lymph nodes. Usually, lymphoma is not localised solely within the salivary glands, but other (cervical) lymph nodes groups are also affected.

CEUS and Elastography

Currently neither CEUS nor elastography have clear indications in the assessment of salivary gland tumours. The results are too variable for this to be considered a reliable clinical tool [(7, 8)]

Pseudo-tumours of the salivary glands

Retention cysts display a smooth outline and are anechoic on ultrasound. Other cysts include cysts of the first branchial arch. The cystic fluid is often echogenic. An unusual type of salivary gland cyst is the so-called ranula. This is a cystic mass arising from the sublingual gland in the floor of the mouth due to obstruction of the ducts of the sublingual gland. Lymphoepithelial cysts may be seen in patients with HIV infection (AIDS) [(9)]. Usually bilateral swelling of the parotid glands is present. Hypertrophy of the masseter muscle is present if a thickness of more than 14 mm in the non-contracted state (transverse diameter) can be measured by ultrasound. Sarcoidosis and tuberculosis can also present as pseudo-tumours (histology is often required to make a definite diagnosis). Lesions of the skin such as sebaceous cysts and other subcutaneous masses are accurately localised sonographically in the subcutaneous tissues.

Ultrasound guided biopsy of the salivary glands

Recent literature states that ultrasound guided core biopsy of the salivary glands is a safe and accurate investigation particularly for the histological diagnosis of tumours. However, while some surgical authors fear that tumour seeding may occur following biopsy, there is no significant evidence base to contradict the view that ultrasound guided fine needle aspiration (FNA) and ultrasound guided core biopsy for salivary tumours is a cost effective and accurate procedure with minimal risk of complications.

Soft tissue lesions of the neck

A detailed knowledge of the anatomy of the soft tissues of the neck is mandatory for the adequate sonographic assessment of the neck. Lesions of the thyroid and parathyroid glands are not covered in the following review.

Cervical cysts

Thyroglossal duct cysts

Thyroglossal duct cysts can arise along a line from the foramen caecum in the base of the tongue to the pyramidal lobe of the thyroid gland. They are usually found in the region of the hyoid bone and at this level are typically midline and are sometimes multilocular. In an infrahyoid location they are typically located off midline, i.e. paramedian. Sonographically thyroglossal duct cysts may be identified as anechoic masses with posterior acoustic enhancement [Figure 12]. However, debris in cysts may simulate a pseudo solid, hypoechoic structure. Following infection, these cysts are usually heterogeneous in echotexture. If the thyroglossal duct cyst is closely related to the hyoid bone or is abutting the hyoid bone, this should be reported as this is important information if surgery is being planned. Rarely a papillary carcinoma can arise within thyroglossal duct cysts.

Figure 12 Longitudinal section of the pre-epiglottic space. An ovoid cystic lesion is seen caudal to the hyoid bone, a thyroglossal duct cyst.

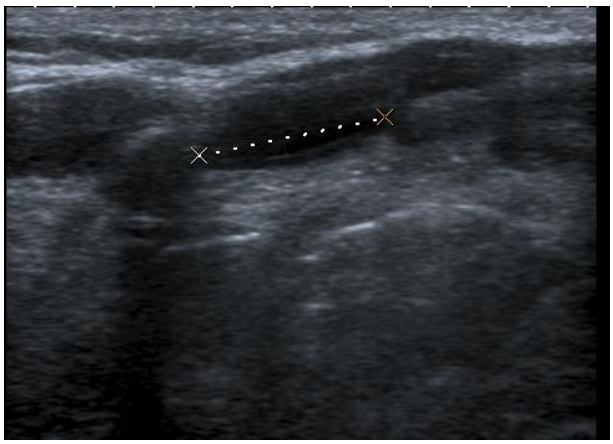

Branchial cleft cysts

These cysts are found in the lateral neck and usually arise from the 2nd or 3rd branchial cleft. The second branchial cleft cyst is the most common congenital cyst presenting in the neck. Usually they are located anterolateral to the carotid bifurcation. Cervical cysts from the first branchial cleft arches can be localised in the parotid region. The echogenicity of branchial cleft cysts varies. Some of these cysts are anechoic. Most, however, contain finely dispersed, homogeneous, echogenic material, the presence of cholesterol crystal aggregates contributing to the echogenic and 'pseudo solid' appearance [Figure 13] [(10)].

In some cases, the mobility of the contents of the cyst can be documented by sonopalpation. Less commonly a fluid/fluid level is detectable. In superadded infection, the fluid within the cyst is typically echogenic and the cyst wall is irregularly thickened. When infection is present there may be associated enlarged regional lymph nodes. No colour flow Doppler signals are found in branchial cleft cysts. If colour flow is identified this indicates a solid lesion. A metastatic squamous cell carcinoma lymph node mass should be considered as a differential diagnosis.

Figure 13 Longitudinal section of the carotid triangle. A 'pseudo solid' homogenous lesion is visualised. Typical branchial cleft cyst.

Dysontogenetic tumours

Epidermoid and dermoid cysts are predominantly located in the midline. The floor of the mouth is regarded as a typical location. Lateral locations, e.g. the parotid glands, are rare. Larger teratomas are sometimes diagnosed in utero. Dysontogenetic cysts often are very echogenic. This is due to the high acoustic impedance of the contents of hair, skin and fluid and sebaceous material. Calcification is typically seen in teratomas.

Lipomas

Lipomas are typically located within the subcutaneous tissues; however, they may occasionally be intramuscular. They are iso- or hyperechoic with a striped or feathered structure. Lipomas are usually ovoid in shape [Figure 14]. While typically located superficially, occasionally cervical lipomas may be identified within the deeper tissues of the neck [(11)]. Multiple lipomata of the neck is sometimes present in patients with alcoholism (Madelung's disease).

Figure 14 An ovoid isoechoic lesion with a feathered structure is seen. Typical appearances of a cervical lipoma.

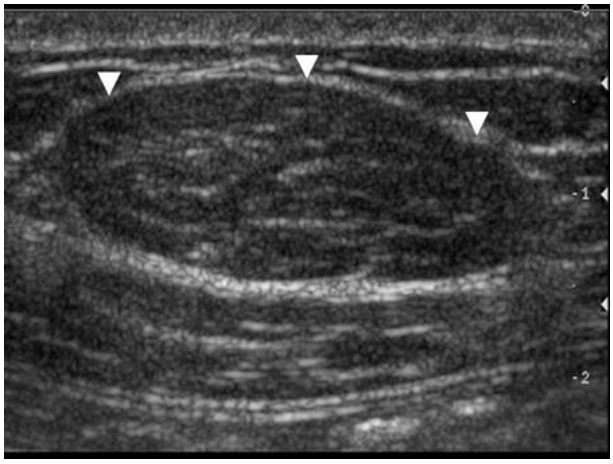

Carotid body tumour

Carotid body tumours are typically located within the carotid bifurcation [Figure 15]. Arteriovenous shunting with high diastolic flow is often identified in these paragangliomas. The blood supply arises from the external carotid artery [(12)]. These non-chromaffin paragangliomas may also originate from the ganglia of the vagus nerve or internal jugular vein. However, glomus jugulare tumours cannot be delineated by sonography due to their superior location, i.e. just inferior to the skull base.

Figure 15 Transverse section of the carotid bifurcation (blue). A vascular solid tumour is seen between the internal carotid artery and the external carotid artery, diagnosed as a carotid body tumour.

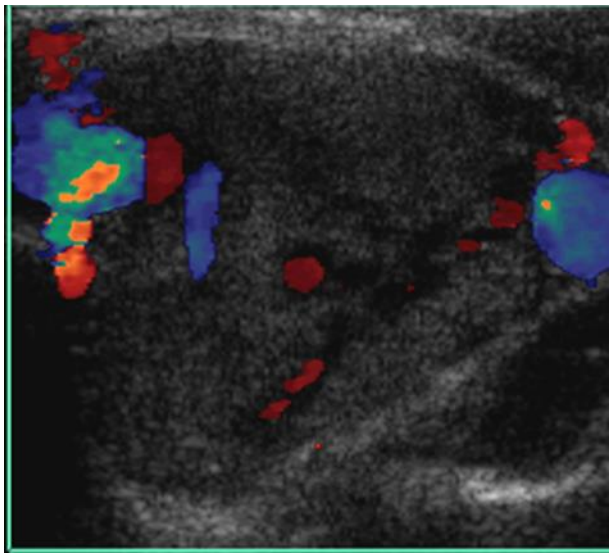

Neurogenic tumours

Neurogenic tumours (neurofibromas and schwannomas) arise from the multiple nerves present within the neck [Figure 16], frequently arising from the brachial plexus or the vagus nerve. The diagnosis can be made when a nerve is identified entering and leaving an ovoid solid lesion. Neurogenic tumours are moderately vascularised on colour Doppler.

Figure 16 Longitudinal section of the brachial plexus. Typical neurogenic tumour (schwannoma) arising from the fascicles of the brachial plexus.

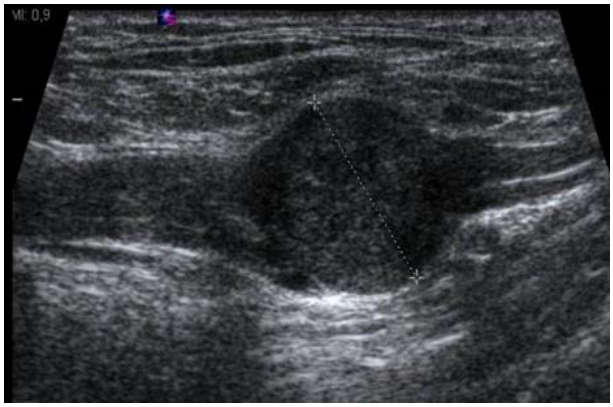

The differential diagnosis of highly vascularised, solid, extrathyroidal lesions include ectopic thyroid gland, paragangliomas, lymph node metastases (especially thyroid cancer or lymphoma) and neurogenic tumours. In children an ectopic thymus and vascular malformations should be considered.

Haemangiomas and lymphangiomas

Large haemangiomas and lymphangiomas [Figure 17] can be diagnosed prenatally by ultrasound. Postnatally, they predominantly occur in the first two years of life. The echogenicity of haemangiomas varies depending on the histology (capillary, mixed or cavernous). Echogenicity is dependent on the size of the cystic cavities. If these cavities are small, the echogenicity of the lesion is increased. Typically, haemangiomas are easily compressible. Associated phleboliths are sometimes detected. Arteriovenous shunts with high diastolic flow may be detected. A lack of detectable blood flow does not exclude a haemangioma, because either the flow may be too slow to be detected by colour Doppler or because the vessels are thrombosed.

Figure 17 Transverse section of the masseter muscle reveals a hypoechoic, compressible vascular mass; a haemangioma.

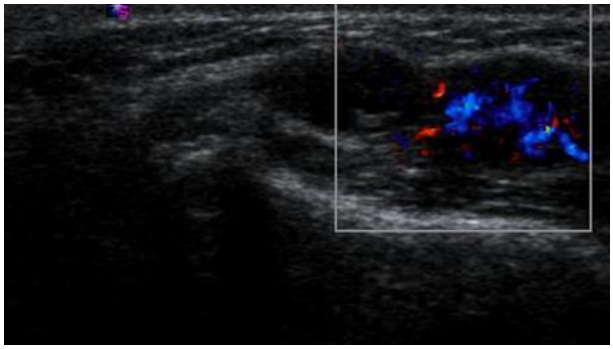

Lymphangiomas (also known as cystic hygromas) are usually found in the early years of life. They are hypoechoic, multicystic lesions with thin septae (i.e. occupy multiple spaces/compartments within the neck) with an absence of identifiable colour Doppler flow signal [Figure 18] [(13)].

Figure 18 Hypoechoic, septated, compressible lesion with no detectable flow on colour Doppler assessment. Lymphangioma of the neck was histologically proven.

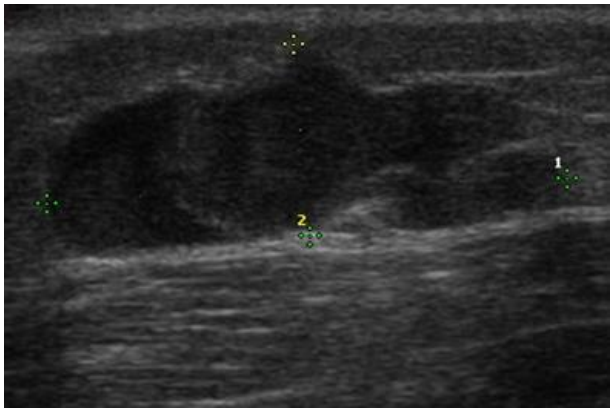

Cervical lymph nodes

In the majority of patients, lymph nodes will be identified within the neck on ultrasound. However, because of the low acoustic impedance differences between lymph nodes and the surrounding soft tissues, normal lymph nodes may be difficult to detect [(14)(15)]. The typical sonographic appearance of a reactive lymph node is that of an ovoid, well-circumscribed hypoechoic lesion. In addition to the oval or elongated (sausage or bean shaped) configuration, an eccentric, echogenic hilum is characteristic of a benign reactive lymph node [Figure 19].

Figure 19 A longitudinal image of a reactive lymph node with an eccentric hilum.

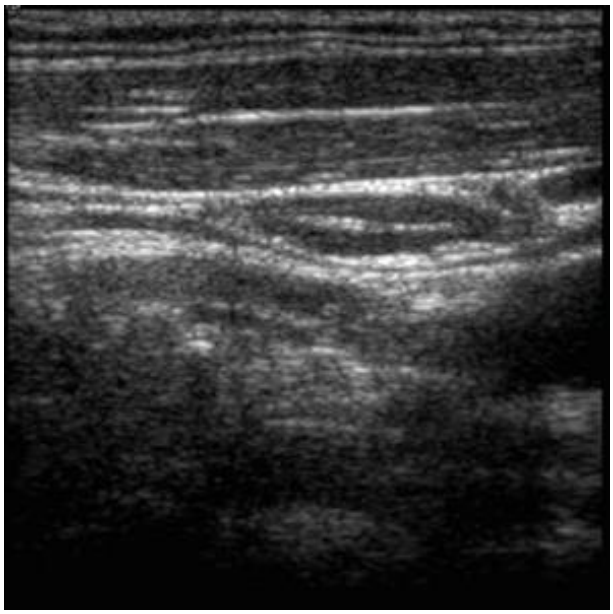

The echogenic hilum is due to hilar blood vessels, the parallel arrangement of lymphoid sinuses within the medulla of the lymph node and fat in the vicinity of the hilum. The longitudinal, i.e. long axis diameter of reactive lymph nodes can be >20 mm. The short axis diameter in the upper internal jugular group can be up to 10 mm, in other sites it is usually <8 mm. The longitudinal diameter, i.e. long axis measurements of lymph nodes in the neck is variable. Children typically have multiple detectable lymph nodes and in contrast to adult cervical lymph nodes they are more bulky (i.e. more rounded or ovoid in shape). This is due to the fact that children have a greater volume of lymphatic tissue compared to adults.

Inflammatory lymph nodes

Viral or bacterial infections are common causes of cervical lymphadenopathy. Most infections cause painful lymphadenopathy. In these cases, imaging is not usually carried out. If there is clinical concern ultrasound can be used for follow-up to assess response during anti-inflammatory therapy.

An annotated diagram of the neck lymph nodes identifying where they are located can be helpful for documentation. Another indication for ultrasound assessment is to diagnose or exclude abscess formation. In the early stages, cystic change is identified within lymph nodes developing suppurative lymphadenitis. Abscesses are usually hypoechoic but may contain echogenic pus. Colour flow imaging may be useful in identifying areas of necrosis with a corresponding lack of colour flow detectable within. Lymph nodes are usually enlarged in bacterial or viral lymphadenitis. Their short axis diameter is often >10 mm and their shape is ovoid to round [Figure 20].

Figure 20 A small ovoid node with hilar vascularity. A typical reactive lymph node is visualised.

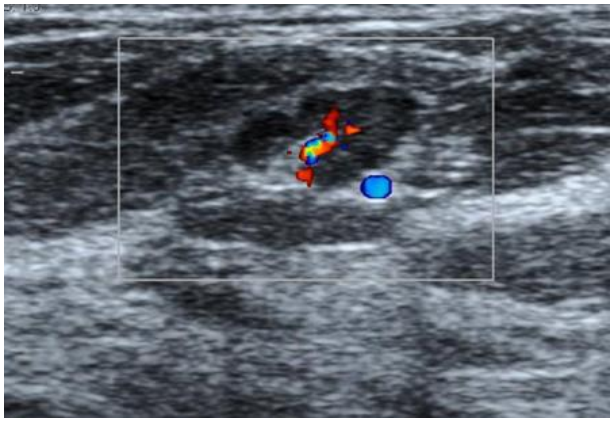

Inflammatory or reactive lymph nodes usually possess smooth or sharp borders. In some cases, there is an eccentric bulging of the lymph cortex. The hyperechoic hilum may be lost, although it is not universally identified in benign lymph nodes. On colour Doppler flow imaging, inflamed lymph nodes have a hilar vascular supply with a regular branching pattern

of the intranodal vessels [Figure 21]. Precise quantification of the increased perfusion using colour Doppler or power Doppler is not necessary.

Figure 21 An ovoid lymph node with a benign hilar blood flow pattern is seen in lymphadenitis.

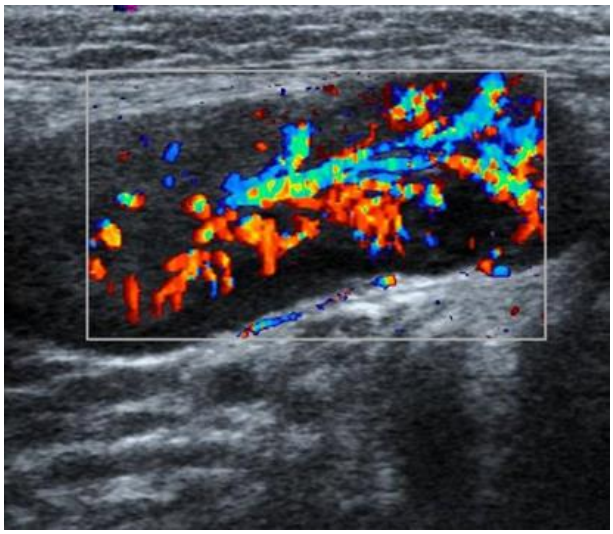

Tuberculous lymphadenitis

Fistula formation is a typical manifestation of tuberculous lymphadenopathy which are identified as connecting hypoechoic structures [(16)]. In the subacute stage, lymph nodes are hyperechoic and heterogeneous in echotexture. The lymph nodes are often poorly vascularised or have no demonstrable colour flow. In the chronic and post-treatment phase, echogenic or calcified areas can be found within the lymph nodes. In the acute stage of tuberculous lymphadenitis, the ultrasound appearances are non-specific. Ovoid to round hypoechoic enlarged lymph nodes are found and differentiation from other nodal adenopathies in the acute stage is not possible. After several weeks, the appearances change and ultrasound examination shows an ill-defined, heterogeneous node. The surrounding fascia is indistinct or blurred and matting of the nodes may be present [Figure 22] [(17)].

Figure 22 A hypoechoic lesion undergoing necrosis with an associated fistula secondary to an underlying diagnosis of tuberculosis.

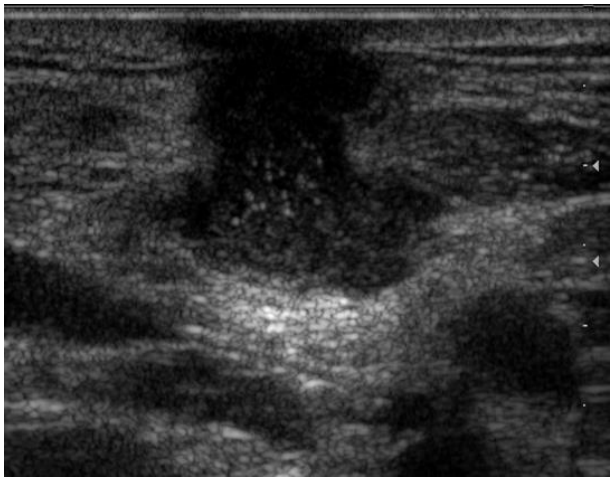

Lymph node metastases

Cervical lymph node assessment and staging in head and neck cancers is an important indication for ultrasound imaging. About 90% of cervical lymph node metastases are due to squamous cell carcinoma. Other common primary tumours that metastasise to cervical lymph nodes are thyroid, breast, lung, stomach and melanoma. It should be noted that the retropharyngeal lymph node group cannot be evaluated by sonography. These nodes however, are only usually involved in pharyngeal cancers, after neck dissection or following radiotherapy. An important criterion for metastatic lymph nodes is a round shape [Figure 23] [(16, 18)].

Figure 23 A rounded lymph node with multiple peripheral arteries is visualised in a squamous cell carcinoma lymph node metastasis.

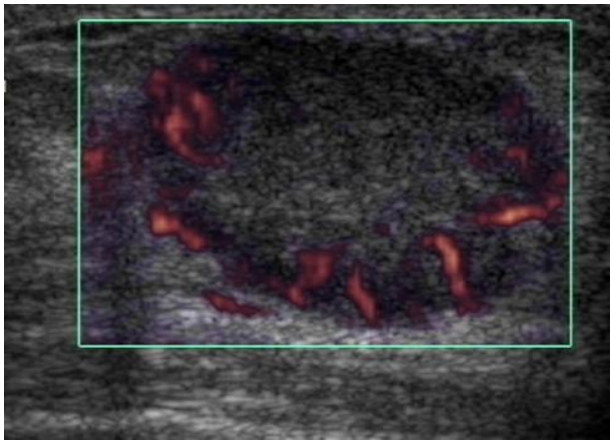

Many authors have emphasised the importance of the ratio of longitudinal to short axis diameter (L/S index). A L/S index of >2 corresponds to a benign lymphadenopathy with an accuracy of 84%, an index of <1.5 was found in 71% of the cases with a metastasis. The short axis diameter is an important criterion in its application to the shape of the node, the rounder the node the more likely it is to be malignant. In patients with a known primary tumour, a short axis diameter of greater than 8 mm is considered suspicious for a metastasis [(19)].

In the carotid triangle or the upper internal jugular chain a short axis diameter of up to 10 mm may be caused by reactive lymph nodes. However, the evaluation of the echo structure, shape and architecture is perhaps the more important criteria for malignant infiltration, in particular in squamous cell lymph node metastatic disease.

Many authors have also used colour Doppler and power Doppler and elastography [Figure 23] to evaluate lymph node metastases [(20)]. Feature of a benign colour flow pattern are a predominantly central blood flow pattern with a hilar vessel communicating with multiple branches [(21)], whereas a chaotic network of intranodal vessels is considered typical for metastatic nodes [Figure 24]. Areas of vascular sparing and multiple peripheral arteries (feeder or subcapsular arteries) are regarded as suspicious for metastatic disease. The areas of vascular sparing are said to correlate with areas of necrosis [(22)].

Figure 24 Rounded lymph nodes with areas of vascular sparing seen in squamous cell carcinoma metastases.

Whilst the sensitivity of ultrasound for the detection of lymph node metastases is good, the specificity of ultrasound alone is limited. However, ultrasound guided fine needle aspiration and ultrasound guided core biopsy allows for excellent differentiation between inflammatory/reactive and metastatic lymph nodes. Nonpalpable lymph nodes can be routinely sampled under ultrasound guidance.

In clinically negative necks of patients with head and neck cancer (N0), the use of ultrasound and ultrasound guided FNA is able to reduce the number of neck dissections performed. It should be remembered that micrometastases may not be detected [(23)].

Sonography is used in the evaluation of suspected infiltration of the great vessels of the neck. In particular, infiltration of the wall of the carotid artery is of significant clinical importance. Detectable contact between the tumour and artery wall of more than 3.5 cm is highly suggestive of infiltration of the deep layers of the artery wall. Sonopalpation, i.e. a gentle bouncing motion with the probe, is recommended for assessing the internal jugular vein to assess infiltration of the vein by tumour. A normal vein will be easily compressible and sonopalpation ensures that the operator identifies a patent internal jugular vein [(24)].

Ultrasound can also be used to document the effects of radio- and chemotherapy on lymph node metastases. Squamous cell lymph node recurrences tend to arise predominantly in the first two years post diagnosis. In selected patients, ultrasound follow-up examinations are necessary to enable the diagnosis of subclinical metastases. The recommended scanning

interval in the first year is between 6 to 12 weeks (depending on the capacity of the ultrasound service). Post neck dissection, tumour recurrence does not follow the established lymph node route of spread as it does in the untreated neck. A diligent search for contralateral metastases and skip metastases is required.

Malignant lymphoma

Histology can differentiate between non-Hodgkin and Hodgkin lymphoma, however ultrasound cannot make that distinction. In most cases of malignant lymphoma at least one or more lymph node groups is affected and in particular the posterior cervical triangle region is commonly involved [Figure 26]. There is often a conglomerate of enlarged lymph nodes. As with sarcoidosis, a so-called facet forming sign may be present. The nodes are round or polygonal in shape and are usually sharply defined. Extranodal infiltrations are rare in lymphoma. In aggressive forms of lymphoma, perinodal fluid collections or oedema is detected and associated matting may be present. The lymph nodes are often very hypoechoic, the so-called ‘pseudocystic’ sign [(25)]. Often small, moderately echogenic structures with a stippled or reticular appearance are found within the lymph node. In some cases a moderate posterior acoustic enhancement is visualised, again in keeping with the 'pseudocystic' sign [(26)]. Necrosis in the strict sense is uncommon in lymphoma. Occasionally echogenic vessel walls of intranodal vessels will be detected. This is called a small-vessel sign [Figure 25]. The architecture of the node is infrequently disrupted in lymphoma and hence the hilum of the lymph node may still be visible [(27)].

Figure 25 Small vessel sign in malignant lymphoma.

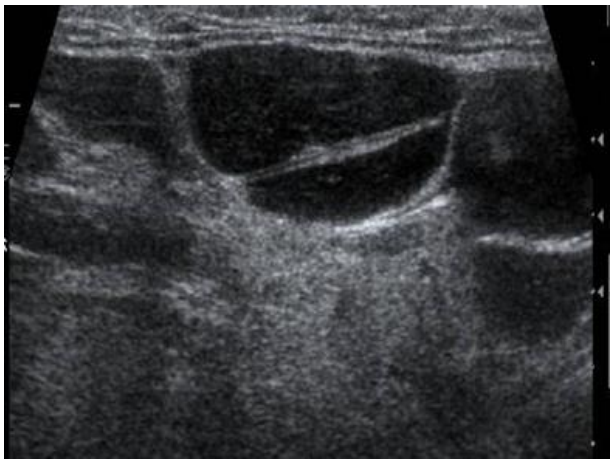

Figure 26 A conglomerate of nodes is visualised in the posterior triangle of the neck in malignant lymphoma.

In Doppler sonography malignant lymphomas often demonstrate a plethoric, benign type, hilar blood flow pattern [(27)] with regular branching of the intranodal vessels [Figure 27]. The chaotic vessel network identified in metastatic squamous cell carcinoma is not typically demonstrated. On colour flow imaging, one cannot distinguish inflammatory nodes from lymphoma.

Figure 27 Power Doppler demonstrates a plethoric hilar flow pattern in non-Hodgkin lymphoma.

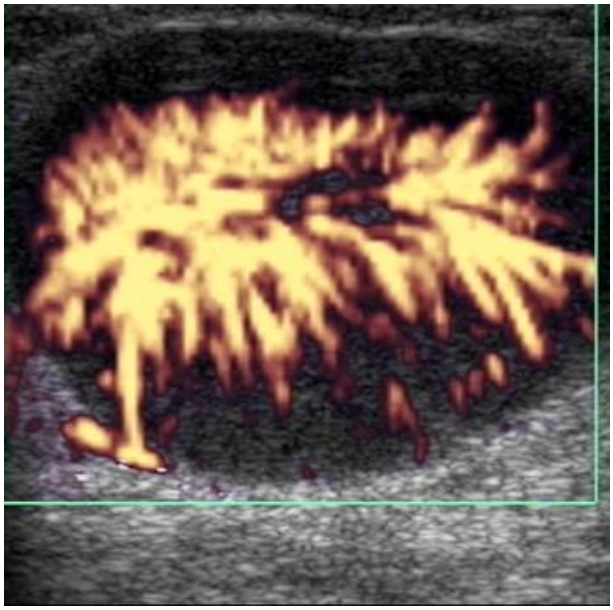

Unusual cervical lymphadenopathies

There are multiple conditions that may mimic lymphoma. Rosai Dorfmann disease is a histiocystosis of the lymph nodes. In this disease the hilar structures are often preserved, however completely hypoechoic nodes may also be present. Kimura's disease (eosinophilic hyperplastic lymphogranuloma) [(26)] and Kikuchi's disease are lymphadenopathies that also present with enlarged hypoechoic lymph nodes [(26, 28)].

CEUS and elastography in cervical lymphadenopathies

Up to now no definitive indications for CEUS and elastography in the assessment of cervical lymphadenopathies have been established [(29-33)].

Summary

High-resolution ultrasound is now the primary imaging method for the evaluation of the soft tissues of the head and neck region. In lymph node assessment, it is able to demonstrate the

morphology of the lymph nodes and is an accurate tool for staging the neck in patients with head and neck cancer. Ultrasound guided biopsy is a safe and cost effective technique allowing either a cytological or histological diagnosis to be obtained.

Other lesions in the neck, e.g. branchial cleft cysts, lipomas, carotid body tumours etc., show a typical sonomorphology which allows an effective imaging triage with ultrasound. For salivary gland masses, ultrasound is frequently the first and often the only imaging modality that is required. Ultrasound can efficiently diagnose the majority of salivary tumours, it allows an ultrasound guided biopsy to be performed and can identify those cases that may require further imaging.

Ultrasound has a key role in the diagnosis of common conditions presenting in the head and neck area when performed by an operator with knowledge of the key anatomy and ability to detect the relevant diagnostic signs.

References

1. Martinoli C, Derchi LE, Solbiati L, Rizzatto G, Silvestri E, Giannoni M. Color Doppler sonography of salivary glands. AJR Am J Roentgenol 1994;163:933-941.

2. Gritzmann N. Sonography of the salivary glands. AJR Am J Roentgenol 1989;153:161-166.

3. Martinoli C, Giovagnorio F, Pretolesi F, Derchi LE. Identification of feeding arteries to establish the intra- or extraparotid location of jugulodigastric nodules: value of color Doppler sonography. AJR Am J Roentgenol 2000;175:1357-1360.

4. Takagi Y, Kimura Y, Nakamura H, Sasaki M, Eguchi K, Nakamura T. Salivary gland ultrasonography: can it be an alternative to sialography as an imaging modality for Sjogren's syndrome? Ann Rheum Dis 2010;69:1321-1324.

5. Feld R, Nazarian LN, Needleman L, Lev-Toaff AS, Segal SR, Rao VM, Bibbo M, et al. Clinical impact of sonographically guided biopsy of salivary gland masses and surrounding lymph nodes. Ear Nose Throat J 1999;78:905, 908-912.

6. Gritzmann N, Macheiner P. [Lipoma in the parotid gland: typical US and CT morphology]. Ultraschall Med 2003;24:195-196.

7. Zhang YF, Li H, Wang XM, Cai YF. Sonoelastography for differential diagnosis between malignant and benign parotid lesions: a meta-analysis. Eur Radiol 2018.

8. David E, Cantisani V, De Vincentiis M, Sidhu PS, Greco A, Tombolini M, Drudi FM, et al. Contrast-enhanced ultrasound in the evaluation of parotid gland lesions: an update of the literature. Ultrasound 2016;24:104-110.

9. Martinoli C, Pretolesi F, Del Bono V, Derchi LE, Mecca D, Chiaramondia M. Benign lymphoepithelial parotid lesions in HIV-positive patients: spectrum of findings at gray-scale and Doppler sonography. AJR Am J Roentgenol 1995;165:975-979.

10. Gritzmann N. Sonography of the neck: current potentials and limitations. Ultraschall Med 2005;26:185-196.

11. Gritzmann N, Schratter M, Traxler M, Helmer M. Sonography and computed tomography in deep cervical lipomas and lipomatosis of the neck. J Ultrasound Med 1988;7:451-456.

12. Gritzmann N, Herold C, Haller J, Karnel F, Schwaighofer B. Duplex sonography of tumors of the carotid body. Cardiovasc Intervent Radiol 1987;10:280-284.

13. Dubois J, Garel L, Abela A, Laberge L, Yazbeck S. Lymphangiomas in children: percutaneous sclerotherapy with an alcoholic solution of zein. Radiology 1997;204:651-654.

14. Ying M, Ahuja A. Sonography of neck lymph nodes. Part I: normal lymph nodes. Clin Radiol 2003;58:351-358.

15. Baatenburg de Jong RJ, Rongen RJ, Lameris JS, Harthoorn M, Verwoerd CD, Knegt P. Metastatic neck disease. Palpation vs ultrasound examination. Arch Otolaryngol Head Neck Surg 1989;115:689-690.

16. Ahuja A, Ying M. Sonography of neck lymph nodes. Part II: abnormal lymph nodes. Clin Radiol 2003;58:359-366.

17. Ying M, Ahuja AT, Evans R, King W, Metreweli C. Cervical lymphadenopathy: sonographic differentiation between tuberculous nodes and nodal metastases from non-head and neck carcinomas. J Clin Ultrasound 1998;26:383-389.

18. van den Brekel MW, Stel HV, Castelijns JA, Nauta JJ, van der Waal I, Valk J, Meyer CJ, et al. Cervical lymph node metastasis: assessment of radiologic criteria. Radiology 1990;177:379-384.

19. Gritzmann N, Czembirek H, Hajek P, Karnel F, Turk R, Fruhwald F. [Sonography in cervical lymph node metastases]. Radiologe 1987;27:118-122.

20. Ahuja A, Ying M, Yuen YH, Metreweli C. Power Doppler sonography to differentiate tuberculous cervical lymphadenopathy from nasopharyngeal carcinoma. AJNR Am J Neuroradiol 2001;22:735-740.

21. Tschammler A, Ott G, Schang T, Seelbach-Goebel B, Schwager K, Hahn D. Lymphadenopathy: differentiation of benign from malignant disease--color Doppler US assessment of intranodal angioarchitecture. Radiology 1998;208:117-123.

22. Rubaltelli L, Khadivi Y, Tregnaghi A, Stramare R, Ferro F, Borsato S, Fiocco U, et al. Evaluation of lymph node perfusion using continuous mode harmonic ultrasonography with a second-generation contrast agent. J Ultrasound Med 2004;23:829-836.

23. van den Brekel MW, Castelijns JA, Stel HV, Golding RP, Meyer CJ, Snow GB. Modern imaging techniques and ultrasound-guided aspiration cytology for the assessment of neck node metastases: a prospective comparative study. Eur Arch Otorhinolaryngol 1993;250:11-17.

24. Gritzmann N, Grasl MC, Helmer M, Steiner E. Invasion of the carotid artery and jugular vein by lymph node metastases: detection with sonography. AJR Am J Roentgenol 1990;154:411-414.

25. Ahuja AT, Ying M, Yuen HY, Metreweli C. 'Pseudocystic' appearance of non-Hodgkin's lymphomatous nodes: an infrequent finding with high-resolution transducers. Clin Radiol 2001;56:111-115.

26. Ahuja A, Ying M, Mok JS, Anil CM. Gray scale and power Doppler sonography in cases of Kimura disease. AJNR Am J Neuroradiol 2001;22:513-517.

27. Vassallo P, Wernecke K, Roos N, Peters PE. Differentiation of benign from malignant superficial lymphadenopathy: the role of high-resolution US. Radiology 1992;183:215-220.

28. Ying M, Ahuja AT, Yuen HY. Grey-scale and power Doppler sonography of unusual cervical lymphadenopathy. Ultrasound Med Biol 2004;30:449-454.

29. Dudea SM, Botar-Jid C, Dumitriu D, Vasilescu D, Manole S, Lenghel ML. Differentiating benign from malignant superficial lymph nodes with sonoelastography. Med Ultrason 2013;15:132-139.

30. Rubaltelli L, Beltrame V, Scagliori E, Bezzon E, Frigo AC, Rastrelli M, Stramare R. Potential use of contrast-enhanced ultrasound (CEUS) in the detection of metastatic superficial lymph nodes in melanoma patients. Ultraschall Med 2014;35:67-71.

31. Poanta L, Serban O, Pascu I, Pop S, Cosgarea M, Fodor D. The place of CEUS in distinguishing benign from malignant cervical lymph nodes: a prospective study. Med Ultrason 2014;16:7-14.

32. Bhatia KS, Lee YY, Yuen EH, Ahuja AT. Ultrasound elastography in the head and neck. Part I. Basic principles and practical aspects. Cancer Imaging 2013;13:253-259.

33. Bhatia KS, Lee YY, Yuen EH, Ahuja AT. Ultrasound elastography in the head and neck. Part II. Accuracy for malignancy. Cancer Imaging 2013;13:260-276.